Chapter 03

Microstructure based flow stress modelling of superalloy 718

Abstract: In order to get the insights about microstructural changes that occurs under the thermo-mechanical processing conditions, the physics based modelling approach is very useful. Therefore, the flow curves of alloy 718 are theoretical simulated using a dislocation density dependent constitutive model for different conditions. Presented model considers the microstructural ingredients that are immobile dislocation density, effective grain size and dislocation cell size as the variables to address the flow curve. The simulated flow curves show a good agreement with the experimental flow curves. The magnitude of immobile dislocation density and dislocation cell size in between 3.87×10^{14} - 3.87×10^{14} m^{-2} and 8.29-8.45 μm, respectively, at the completion of the simulation. Furthermore, this approach also provides the possibility to quantify and depict the variation in each strengthening contributions.

3.1. Introduction

IN 718 alloy is an important nickel-based superalloy that can be used to fabricate the components of power plants and jet engines, due to its excellent high temperature deformation and oxidation resistance. The microstructure of the alloy changes as a result of thermo-mechanical processing (TMP) like rolling, forging etc. In order to get the insights about microstructural changes that occurs under TMP, one way is to model the stress-strain curves employing physics based approaches. The very first comprehensive models to attempt this task were based on simple empirical descriptions by Holomon [132], Ludwik [133] and Voce [134]. This type of empirical models uses many constants that are without any physical meaning, in synergy with the strain, strain rate and temperature. Later on, the physical models were developed by Mecking et al. [32],

Bergstrom et al. [26, 88], Surya et. al [41], Joseph et al. [91] and many other researchers that rely mostly on different dislocation densities as an internal state variable. The physics based approaches work on the mechanisms that occur inside the materials during the metal working. In order to address the various mechanisms, proper internal variables that are very much dependent on particular material and its processing history, need to be defined precisely.

In this study, we have put forth a sophisticated dislocation density dependent physical model that is constructed on the finding originally by Lindgren's group [3, 34]. Herein, the model development includes the addition of twin boundaries as a strengthening elements as a new addition to previous developed models [3, 34]. The strength of Ni based alloys depends on long-range (LR) and short-range (SR) interactions, solute hardening and dislocation accumulation at different interfaces such as cells, twin boundaries (TBs) and other high angle grain boundaries (HAGBs). Thus, total flow stress in the 718 alloy was considered to be the addition of the LR hardening due to immobile dislocations, modified Hall-Petch effect, which accounts for effective grain size ($g_{eff)}$ due to the presence of twins, the short-range contributions, which take into account general barriers and solute contributions. In order to verify the simulated flow curves, the experimental flow stress curves were collected from the literature [4]. This approach also allows for the comparative assessment of the various strengthening mechanisms contributions, even with ongoing deformation.

3.2. Methodology

The flow curves were adopted from [4] and the chemical composition of precipitate free IN 718 alloy [4] is given as: Ni 53.5, Cr 18.4, Mo 3.05, Nb 5.0, Ti 0.94, Al 0.6, Si 0.08, Co 0.17, Mn 0.11, Cu 0.13, C 0.03, P 0.010, S 0.0004 and Fe balance. The flow curves were collected for the deformed conditions such as at 873 K / 10^{-2} s^{-1} - $10^{-1}s^{-1}$ and 1073 K / 10^{-2} s^{-1} - 10^{-1} s^{-1}. In the

MATLAB software, the differential equations are solved using the Euler method. Initial immobile dislocation density was taken as 1×10^{11} m^{-2} and magnitude of others parameters were taken from the literature to initialize the model [4]. The Appendix 3.A contains the material constants and calibrated model parameters, respectively, for the alloy 718, see Table 3.2 and Table 3.3.

3.3. Model Formulation

In general, the permanent deformation in the IN 718 proceeds via the movement of dislocations. An increase in the number of immobile dislocations is a key indicator of strain hardening in low stacking fault energy materials (LSFE). The change in immobile dislocation density (ρ_i) with respect to time is expressed as [3, 34],

$$\dot{\rho_i}^{(+)} = \left(\frac{1}{s} + \frac{1}{g_{eff}}\right)\frac{M}{b}\dot{\varepsilon}^p, \tag{3.1}$$

g_{eff} is effective grain size and $\dot{\varepsilon}^p$ is plastic strain rate. Herein, the "s" is estimated through the following expression [135],

$$s = \frac{K_c}{\sqrt{\rho_i}}, \tag{3.2}$$

where, k_c is temperature dependent calibrated parameter. The softening mechanisms, i.e., static recovery and dynamic recovery also occurs simultaneously reducing the dislocation density and minimising the elastic stored energy of the system. IN 718 alloy, being the LSFE material, it is reasonable to assume that climb may predominate during static recovery. Nes et al.[136] developed the following expression for static recovery, which considers climbing of dislocations as governing mechanism,

$$\rho_{static\ recovery} = C_{sr}\, D_v \frac{Gb^3}{k_B T}\left({\rho_i}^2 - {\rho_{grwn}}^2\right), \tag{3.3}$$

The immobile dislocation has possibility to interact with the mobile dislocations and may get annihilated leading to dynamic recovery. Dynamic recovery phenomena is already thoroughly discussed in the literature and it can be expressed as [3, 34],

$$\rho_{dynamic\,recovery} = \Psi \rho_i \dot{\varepsilon}^p \tag{3.4}$$

Herein Ψ is a recovery function and expressed as [26]

$$\Psi = \Psi_0 + \Psi_{r0} \left(\frac{D_v}{\dot{\varepsilon}^p b^2}\right)^{\frac{1}{3}} \tag{3.5}$$

where Ψ_0 and Ψ_{r0} are the constants need to be calibrated. The overall/total flow stress can be obtained as the sum of different strength contributions, i.e., from dislocations, Grains and cells, and solid solutions. It can be expressed as,

$$\sigma_{flow} = \sigma_{dis} + \sigma_{HP} + \sigma_{ss}\,, \tag{3.6}$$

Herein, the strengthening contribution from the dislocation is given by Taylor hardening relations [3, 34],

$$\sigma_{dis} = \alpha M G_T b \sqrt{\rho_i} \tag{3.7}$$

Furthermore, by incorporating the twin boundary concept [137], the grain boundary strengthening contribution is calculated using the modified Hall-Petch contribution and is represented as [34],

$$\sigma_{HP} = \frac{K_{HP} G_T}{\sqrt{g_{eff}} G_{RT}} = \frac{K_{HP}\ G_T}{\sqrt{g} G_{RT}} \left[1 + 2K_t ln\left(\frac{g}{g_0}\right)\right]^{\frac{1}{2}} \tag{3.8}$$

Herein g is grain size before annealing, g_0 is grain size after annealing and K_t is a constant. The short range contribution provided by the solid solutions is estimated through the following

expression [138],

$$\sigma_{ss} = \left[\sum_{i=0}^{n} Z_L G(T)^{\frac{3}{2}} \left(\alpha_s \delta_i + \acute{\eta}(T)\right)^2 c_i\right]^{\frac{2}{3}} \quad (3.9)$$

Herein Z_L is a material parameter, c_i is solute concentration α_s is a dimensionless constant and $\acute{\eta}(T)$ is the temperature-dependent misfit. The detailed explanations can be find in the published work of Malmelov et al.[4]. The short range strengthening also inlcudes the strengthening from the orthogonal dislocation interactions. The research work in this chapter excludes the effect of orthogonal dislocation interactions and the short range contribution is only considered due to solid solution strengthening.

3.4. Results and discussion

Figures 3.1a, b , c and d represents the σ_{flow} vs. true plastic strain curves of IN 718 alloy for the conditions that are 873 K / $1.0\times10^{-2.0}$ s^{-1}, 873K / $1.0\times10^{-1.0}$ s^{-1}, 1073 K / $1.0\times10^{-2.0}$ s^{-1} and 1073 K / $1.0\times10^{-1.0}$ s^{-1}. The experimental flow curves are used to validate the predicted flow curves, and they are found to be in agreement. The main contributing factors to the σ_{flow} are dislocation strengthening and Hall-Petch strengthening. The magnitudes for these aforementioned strengthening mechanisms lie in the range 746.60-845.490 MPa and 140.490-158.320 MPa, respectively, at the end of deformation for these investigated conditions.

The experimental and modelled σ_{flow} vs. true plastic strain curves in Figure. 3.1c differ as a result of recrystallization that may occur during the deformation and it can lead to decrease the σ_{flow} during the subsequent deformation. It has to be clarified that recrystallization mechanism is not included in this model. The σ_{flow} consisting the different source of contributions is described in Table 3.1.

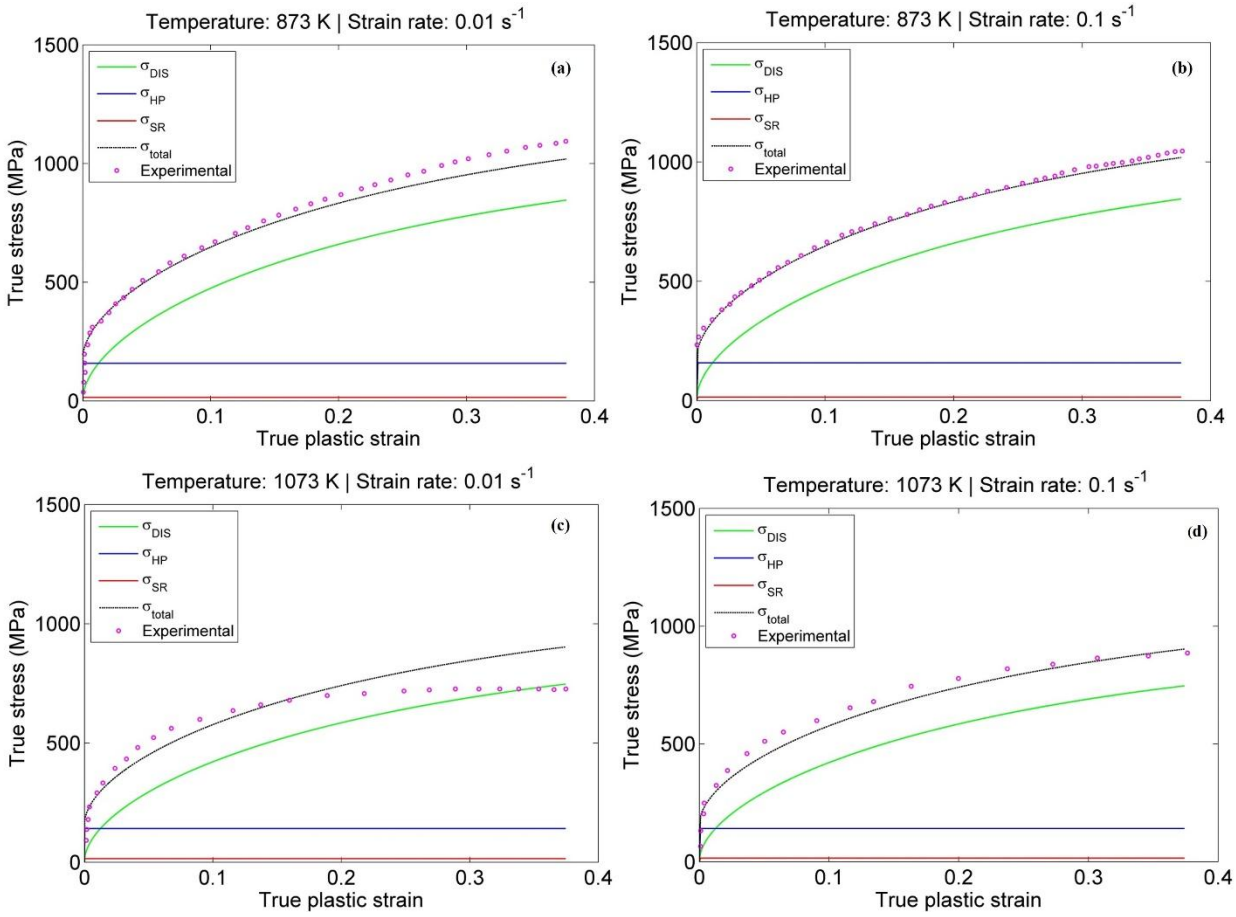

Figure 3.1. σ_{flow} vs. true plastic strain curves of IN 718 alloy with considering the modified Hall-Petch equation incorporating the annealing twin boundaries at 873 K (a) $1.0 \times 10^{-2.0}\ s^{-1}$, (b) $1.0 \times 10^{-1.0}\ s^{-1}$ and at 1073 K (c) $1.0\times10^{-2.0}\ s^{-1}$, (d) $1.0\times10^{-1.0}\ s^{-1}$. Experimental flow curves are taken from Malmelov et al. [4].

Figures 3.2a, b , c and d represent the variation of ρ_i and s with ongoing deformation at 873 K / $1.0\times10^{-2.0}\ s^{-1}$, 873K / $1.0\times10^{-1.0}\ s^{-1}$, 1073 K / $1.0\times10^{-2.0}\ s^{-1}$ and 1073 K / $1.0\times10^{-1}\ s^{-1}$. The predicted magnitude of ρ_i and s falls between 3.81×10^{14} - $3.87\times10^{14.0}\ m^{-2}$ and 8.29-8.45μm, respectively, at the end of simulation for the considered cases. The generation of dislocations and its immobilization causes an increase in the ρ_i and a decrease in s . In case of Haynes 282 alloy, at 815 °C / $1\times10^{-4.0}\ s^{-1}$, ρ_m and ρ_f were reported to be ~$2\times10^{14.0}$ and ~$2\times10^{16.0}\ m^{-2}$, respectively[139]

. Similar to this, Voyiadjis et al. [7] formulated a internal variable dependent constitutive model for IN 718 superalloy that also accounts for dynamic strain ageing in superalloy. At 200 °C/$1.0\times10^{-3.0}$ s^{-1}, the dislocation density is predicted to be ~$24\times10^{13.0}$ m^{-2}.

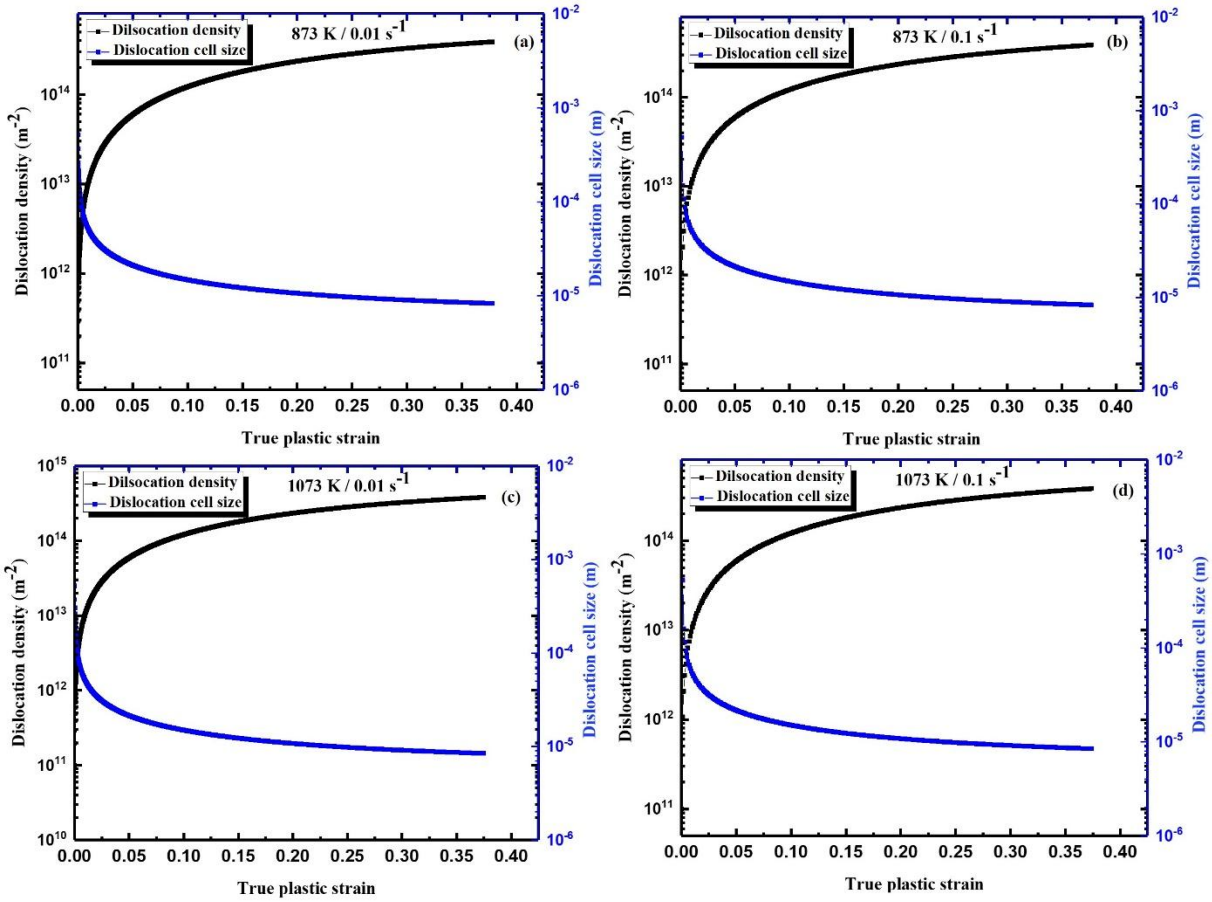

Figure 3.2.Variation of $\boldsymbol{\rho_i}$ and s of IN 718 alloy is plotted with ongoing strain at 873 K (a) $1.0\times10^{-2.0}$ s^{-1}, (b) $1.0\times10^{-1.0}$ s^{-1} and at 1073 K (c) $1.0\times10^{-2.0}$ s^{-1}, (d) $1.0\times10^{-1.0}$ s^{-1}.

Table 3.1. Strength contributions at the end of simulation for different conditions

	873 K / $10^{-2.0}$ s^{-1}	873 K / $10^{-1.0}$ s^{-1}	1073 K / $10^{-2.0}$ s^{-1}	1073 K / $10^{-1.0}$ s^{-1}
σ_{DIS} , (MPa)	845.49	844.93	746.96	746.60
σ_{HP}, (MPa)	158.32	158.32	140.89	140.89
σ_{SS}, (MPa)	014.96	014.96	016.92	016.92

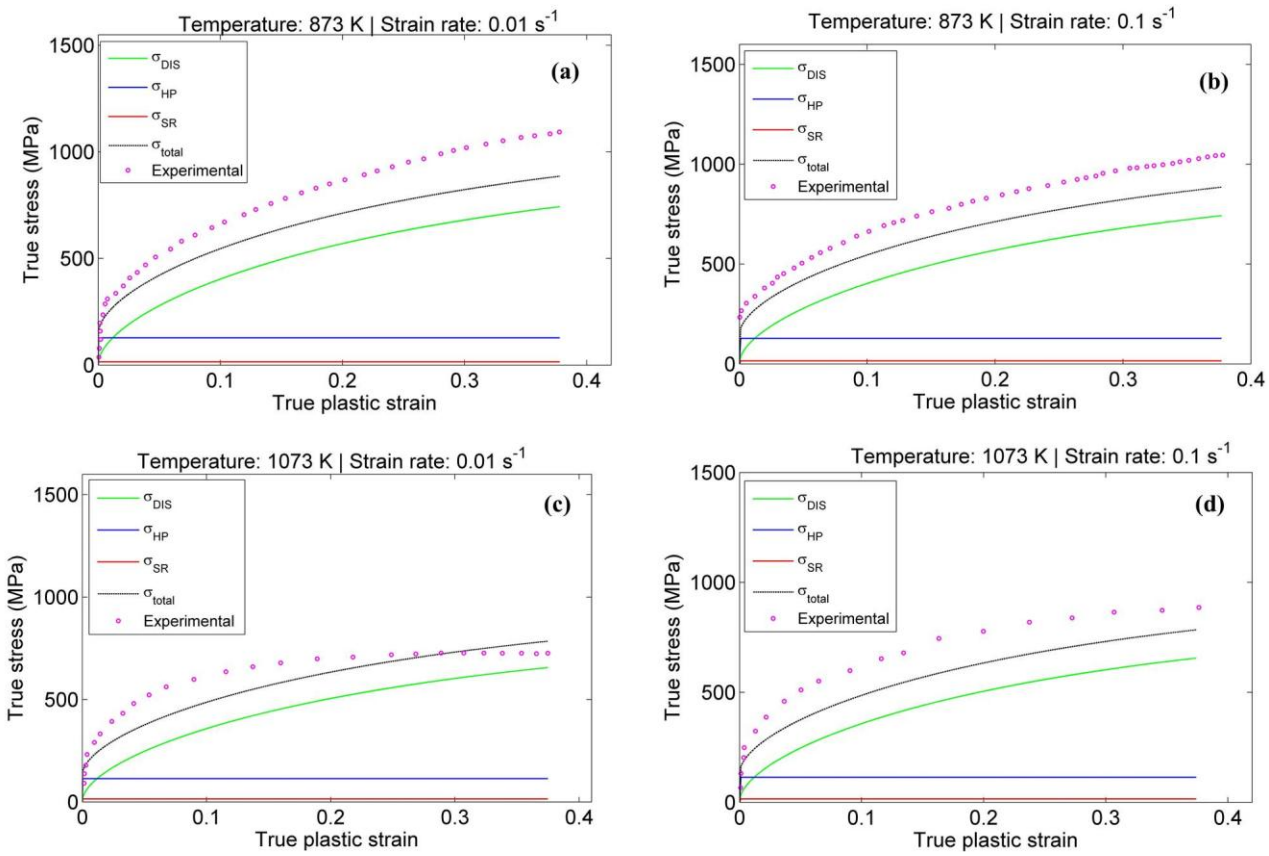

Figure 3.3. σ_{flow} vs. true plastic strain curves of IN 718 alloy using traditional Hall-Petch equation [91] without considering the effect of annealing twins at 873 K (a) $1.0 \times 10^{-2.0}\ s^{-1}$, (b) $1.0 \times 10^{-1.0}\ s^{-1}$ and at 1073 K (c) $1.0 \times 10^{-2.0}\ s^{-1}$, (d) $1.0 \times 10^{-1.0}\ s^{-1}$. Experimental flow curves are taken from Malmelov et al.[4]

Figures 3.3a, b , c and d represent the σ_{flow} vs true strain curves of alloy 718, considering the traditional Hall-Petch equation [91], that does not considers the effect of annealing twin boundaries at 873 K / $1.0\times10^{-2.0}\ s^{-1}$, 873K / $1.0\times10^{-1.0}\ s^{-1}$, 1073 K / $1.0\times10^{-2.0}\ s^{-1}$, and 1073 K / $1.0\times10^{-1.0}\ s^{-1}$. It can be seen that, when the twin boundaries are not included in the model, the predictions of flow responses are not good and there is significant deviation in experimental and predicted flow curves.

3.5. Conclusions

Flow stress response of precipitate free IN 718 was modelled using a physics reliant flow stress model. Both the LR and SR strengthening contributions were considered for predicting the overall flow behavior. The important findings are given below,

- The contributions of dislocation strengthening and Hall-Petch strengthening dominates over others with respect to the overall σ_{flow}. The magnitude of σ_{dis} and σ_{HP} were observed to be in the range of 746.60-845.49 MPa and 140.490-158.320 MPa, respectively.
- At the completion of the numerical computation, the magnitude of ρ_{imm} and s falls between $3.87\times 10^{14.0}$ - $3.87\times 10^{14.0}$ m^{-2} and 8.290-8.450 μm, respectively. The predictions of flow responses are not good and there is significant deviation in experimental and predicted flow curves, if twins are not considered and traditional Hall-Petch equation is used.

Appendix 3.A

Table 3.2. Model parameters taken from the literature

	Magnitude	**Ref.**	**Variable**	**Value**	**Ref.**	**Variable**	**Magnitude**	**Ref.**
g (μm)	20	**[4]**	ρ_{grwn} (m^{-2})	1 x 10^{11}	**[4]**	K_{HP} $(Pa\ m^{1/2})$	0.75 x 10^{3}	**[4]**
b (m)	2.50 x 10^{-10}	**[4]**	*M*	3.06	**[4]**	K_B *(J/K)*	1.38 x 10^{-23}	
$\dot{\varepsilon}_{ref}$	1.00 x 10^{6}	**[4]**	g_0 *(μm)*	~ 9.5	[140]			

Table 3.3. Model calibrated parameters

α	ρ_{i0} (m^{-2})	C_{sr}	Ω_0	Ω_{r0}	K_{c0}	G_0 *(Pa)*	D_G *(Pa)*
1	$1x10^{11}$	$1.5x10^{-4}$	4.5	0	154	$79.1x10^{9}$	$9.132x10^{9}$